scientific reports

Check for updates

OPEN

Investigation of fullerene motion on thermally activated gold substrates with different shapes

Amir Shamloo[1]✉, Mohammad Ali Bakhtiari[1,2], Mahdi Tohidloo[1,2] & Saeed Seifi[1,2]

In the current study, the regime of motion of fullerene molecules on substrates with different shapes at a range of specific temperatures has been investigated. To do so, the potential energy of fullerene molecules was analyzed using the classical molecular dynamics method. C_{20}, C_{36}, C_{50}, C_{60}, C_{72}, C_{76}, C_{80}, and C_{90} fullerene molecules were selected due to their spherical shapes with different sizes. In addition, to completely analyze the behavior of these molecules, different gold substrates, including flat, concave, the top side of the step (upward step), and the downside of the step (downward step) substrates, were considered. Specifying the regime of the motion at different temperatures is one of the main goals of this study. For this purpose, we have studied the translational and rotational motions of fullerene molecules independently. In the first step of the investigation, Lennard-Jones potential energy of fullerene molecules was calculated. Subsequently, the regime of motion of different fullerenes has been classified, based on their displacement and sliding velocity. Our findings indicated that C_{60} is appropriate in less than 5% of the conditions. However, C_{20}, C_{76} and C_{80} molecules were found to be appropriate candidates in most cases in different conditions while they were incompetent only in seven situations. As far as a straight-line movement is considered, the concave geometry demonstrated a better performance compared to the other substrates. In addition, C_{72} indicated less favorable performance concerning the range of movement and diffusion coefficients. All in all, our investigation helps to understand the performance of different fullerene molecules on gold substrates and find their probable application, especially as a wheel in nano-machine structures.

Manipulation of nano-scale materials is becoming increasingly appealing for various technological objectives, thanks to the rapid development of nano-robots. In current years, quite a few transportation mechanisms have been suggested to carry nano-sized particles[1]. However, most of these approaches were incompetent due to several reasons. First, practically all created nano-manipulators are several orders of magnitude larger than their payload, which is contrary to natural nano- manipulators' performance[1,2]. In nature, molecules of the same order of magnitude or even smaller are capable of transporting atoms and molecules. Kinesin, for example, is a small protein that can transport quite large payloads properly[3,4]. Second, they are unable to simultaneously work on a large number of particles[2].

James Tour et al. assembled several molecular motors with the goal of transporting other nano-scale materials[5–9]. These manufactured molecular machines have obtained such names like nanocars, nanotrucks, or other names because of their similarity to real cars among researchers[2,6,10]. Various nano-machines have been developed, each with a different shape and number of wheels. The first generation of synthesized nanocars moved with the aid of fullerene wheels[11,12]. C_{60} is a well-known molecule whose mobility on various substrates has been illustrated in a number of experimental and computational studies[12,13]. In addition, the motion of C_{60} on graphene, silicone, and gold substrates has been studied previously[14–17]. However, fullerene-wheeled nanocars have shown more profitable performance on the gold substrate due to their stability and conductivity[13]. Four or three-wheeled nano-machines with C_{60} as a wheel were fabricated significantly in previous studies of these nano-machines[5]. Vaezi et al.[18] investigated the motion of C_{60} molecule on the boron-nitride substrate at different temperatures. They indicated that as the temperature increased, the rolling motion became more significant than the siding motion, and the range of the movement and diffusion coefficients became greater. Despite the progress made in the study of C_{60}, the regime of motion of other fullerenes has not been investigated in detail. Thus, it seems extensively needed to investigate the mobility of other fullerene molecules on different substrates

[1]School of Mechanical Engineering, Sharif University of Technology, Azadi Ave., Tehran, Iran. [2]These authors contributed equally: Mohammad Ali Bakhtiari, Mahdi Tohidloo and Saeed Seifi. ✉email: shamloo@sharif.ir; shamloo@sharif.edu

to assess their contingent applications. For instance, Wang et al.[19] investigated the motion of C_{60}, C_{72}, C_{180}, C_{240}, and C_{260} fullerenes on the graphene substrate. They demonstrated that all molecules reached the end of the substrate with maximum velocity and started fluctuating at that point. Hence, these molecules may be utilized in the construction of high-frequency nano-switches, nanoparticle transport, or nano-robot components.

It is worthy to note that prior to utilizing these nano-machines, experimental or analytical approaches should be used to determine their class of motion[20]. Scanning Tunneling Microscopy (STM) is an effective measurement technique that has been utilized to monitor a range of nanocars[21]. Shirai et al.[9] and Zhang et al.[20] have employed experimental methods to evaluate the motion of nano-carriers. They studied the mobility of numerous fullerene-wheeled nanocars on a gold substrate at different temperatures. However, STM has a number of disadvantages, such as it requires an expensive and time-consuming process while just a few images can be obtained in a minute and the details of the motion can be partially displayed[22]. As a result, other approaches such as computational simulation can be suitable for measuring the motion of these nano-machines in various situations[23–27]. Akimov et al.[28] and Konyukhov et al.[29,30] simulated a nanocar with rigid C_{60} wheels and rigid chassis using the coarse-grained molecular dynamics method. Even though their simplified assumptions allowed them to perform simulations faster, it is essential to mention that the model precision was reduced in their study resulting in missing the details about the nanocar motion.

In this study, the motion of several fullerene molecules on four different gold substrates has been investigated. C_{20}, C_{36}, C_{50}, C_{60}, C_{72}, C_{76}, C_{80}, and C_{90} fullerene molecules have been selected due to their spherical shapes with different sizes. In addition, to completely analyze the behavior of these molecules, different gold substrates, including flat, concave, the top side of the step (upward step), and the down side of the step (downward step) substrates, were considered. In the first step, the potential energy of fullerene molecules was calculated and then their variation during motion was investigated. Afterwards, the probable motion was predicted in different conditions based on the obtained results. The classical molecular dynamics method has been performed in the second step. The motion of fullerenes has been examined on the thermally induced substrates to achieve a better control over fullerene movement. Modelling the fullerene motion can result in anticipating the movements of fullerene-based nanocars under a myriad of methods.

Methods

Potential energy of fullerenes. Potential energy analysis is a powerful method for predicting the mobility of fullerenes on quite a few substrates. This section investigates the mobility of several fullerenes (Fig. 1) on gold substrates with different shapes (Fig. 2), namely, the flat, upward step, downward step, and concave substrates. The upward and downward step substrates were considered to provide a better control over the motion of fullerene (Fig. 2 B,C). Furthermore, the central part of the concave substrate corresponds to the flat substrate, and its Up and down sides correspond to the downward step and upward step substrates when fullerenes are lowered or raised, respectively (Fig. 2D).

It is worth noting that in calculating the potential energy, fullerene is considered a rigid molecule. It means that the potential energy between the carbon atoms is constant and does not need to be calculated. Thus, the internal potential energy among the carbon atoms of fullerene was ignored, and the potential energy of fullerene stands for the potential energy resulting from the interaction between fullerene's carbon atoms and the gold atoms of the substrate. The rigid molecular structures of all fullerenes were provided from the Nanotube Modeler program in the fullerene library[31]. Some fullerene molecules have many isomers, so we select the one that has a spherical shape like C_{60} (e.g. C_{36} has 15 isomers and we chose the isomer named No.15-D6h.cc1, C_{50} has 271 isomers and we chose the isomer named No.271-D5h.cc1, C_{76} has 2 isomers and we chose the isomer named C76-Td.cc1, C_{80} has 7 isomers and we chose the isomer named No.6-D5h.cc1, and C_{90} has 46 isomers and we chose the isomer named No.20-C1.cc1 based on their spherical shapes, from the nanotube modeler).

According to Pishkenari et al.[32], the potential energy of C_{60} on a gold substrate varies depending on its orientation. They compared four different C_{60} orientations, taking into account translational and rotational motion, and found that the Hexa-down orientation has the most stable motion. Therefore, in the current work for all the aforementioned fullerenes were placed on substrates via their Hexa-down orientation except C20, which was placed on its pentagonal side.

The potential energy of fullerenes was calculated employing Lennard-Jones potential as below (Eq. 1):

$$E_{Lj} = 4\varepsilon\left[\left(\frac{\sigma}{r}\right)^{12} - \left(\frac{\sigma}{r}\right)^{6}\right] \tag{1}$$

where σ, ε, and r are potential parameters that indicate the equilibrium distance of the Au−C bond ($\sigma = 2.9943$Å), the well depth of the potential ($\varepsilon = 0.01273eV$), and the distance between the gold and carbon atoms in an equilibrium location, respectively. In addition,$r_{cut-off}$ represents the cut-off radius for the Lennard-Jones potential and is set to 13Å.

Simulation setup. In the current study, the motion of several fullerene molecules on the gold surfaces with different shapes has been examined using the classic molecular dynamics method. Simulations were performed at different temperatures in the range of $75K$ to $600K$ to investigate the effect of the temperature on the mobility of fullerene molecules. The temperature of the substrate and fullerenes was regulated by employing the Nose–Hoover thermostat. The fullerene molecule was placed on the top of the substrate, while the lower layer was supposed to be rigid. Substrate size was adjusted to $18a \times 18a \times 3a$, where a stands for the gold lattice constant, set to be 4.078 Å. Additionally, periodic boundary conditions were utilized in the x and y directions, and the plane direction of the gold surface was considered to (001) concerning the FCC crystalline direction.

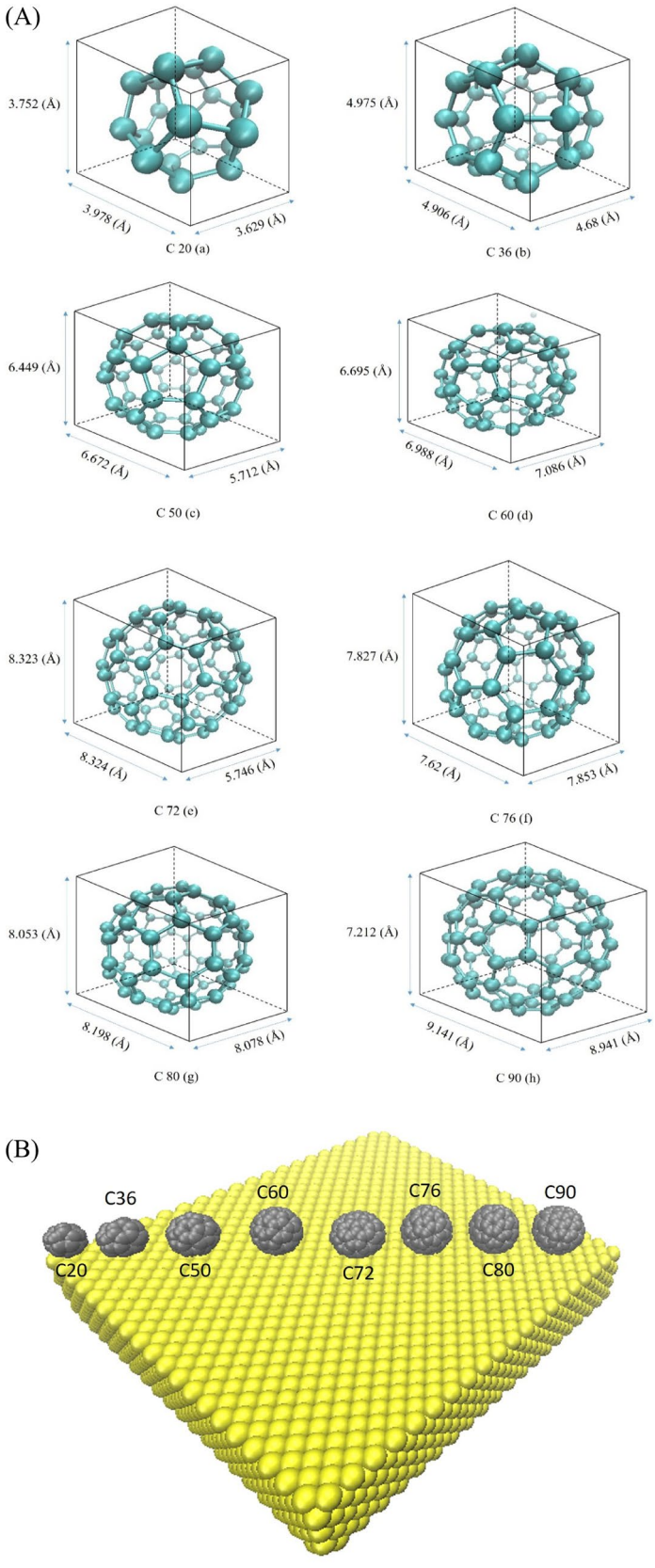

Figure 1. (**A**) The three-dimensional view of Different fullerenes simulated in this study which are C_{20} (a), C_{36} (b), C_{50} (c), C_{60} (d), C_{72}(e), C_{76} (e), C_{80} (d) and C_{90} (h). (**B**) the fullerene molecules contacted from Hexa-Down orientation on the substrate at each starting point.

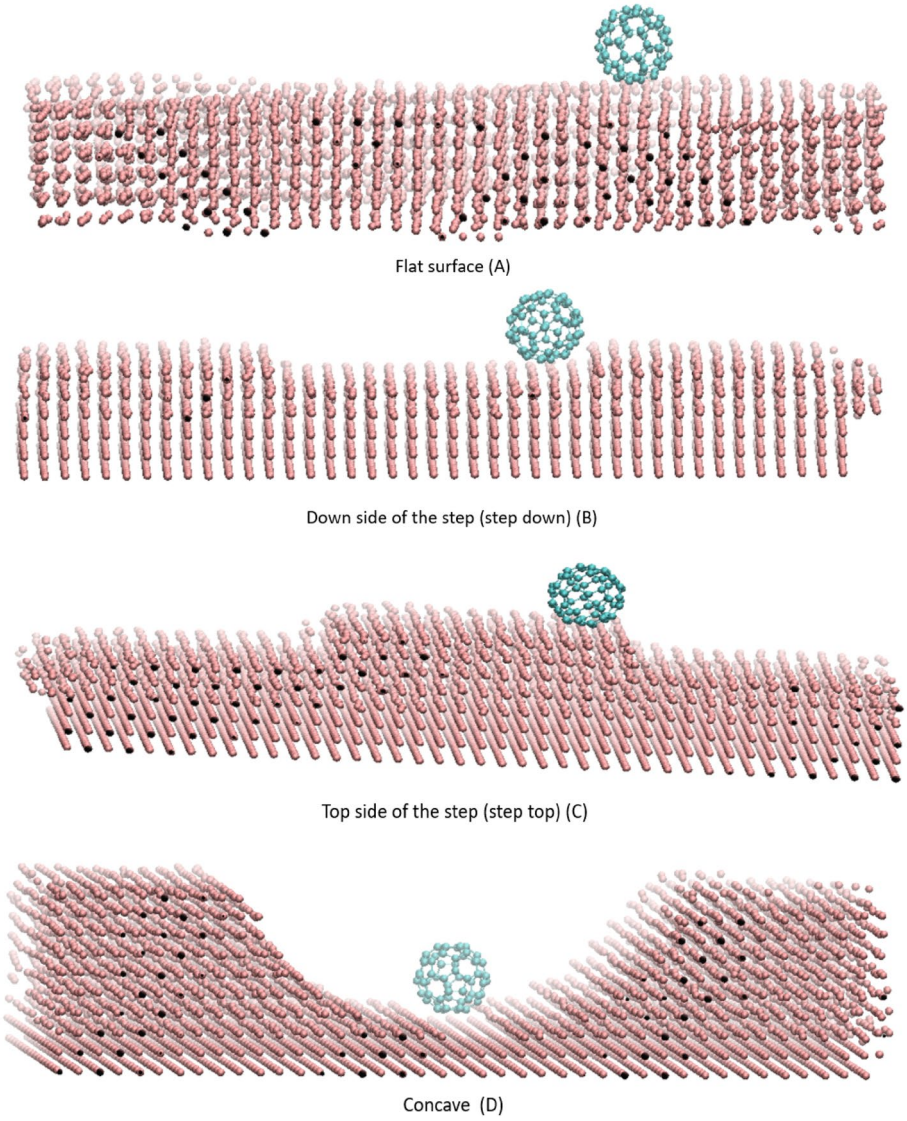

Figure 2. C_{60} fullerene on different gold substrates. (**A**, **B**, **C**, and**D**) representing the Flat surface, Down side of step, Top side of the step, and Concave substrates, respectively.

To model the interaction between the gold atoms in the substrate, the EAM potential was applied[33]. This potential was developed using density functional theory, which is recognized as one of the most accurate potentials for mimicking Au and other FCC metals so far. This potential has been shown to accurately replicate the vacancies and disorders in Au substrates, and the dislocation structures predicted by this potential match with experimental observations properly. Simulations were performed using LAMMPS software[34], and the results are envisioned by operating the VMD package[35]. Before starting the simulation, the system was relaxed for 200,000 steps, and then, the simulation was performed for 8*ns* considering 1*fs* time steps to attain accurate results. The velocity Verlet algorithm was used to integrate the equations of motion with a 1*fs* time step. It is worth mentioning that *Tdamp* is set to 50*fs* in the LAMMPS software for NVT ensemble as well[36].

Results

The main goal of this study is to find the optimal fullerene molecules to be used as a wheel in nano-machines. For this aim, the motion of fullerene molecules on different gold substrates has been analyzed in the first stage. According to the geometries studied in the current investigation, the fullerene molecules have shown more deviation from their direct path on the flat substrate than the other substrates since the motion of the molecules was not restricted on this substrate. After the flat substrate, the most deviation of the fullerene molecules happens on the upward step substrate due to its high-energy points resulting from the surface effects, and no energy is needed to jump down the step. Furthermore, by increasing the radius of the fullerene molecule from C_{20} to C_{90}, it was observed that the range of motion of fullerenes has become smaller due to the generation of more non-bonded forces between the gold substrate and the fullerenes' carbon atoms (Figs. 3, 4 and 5 blue and gray lines).

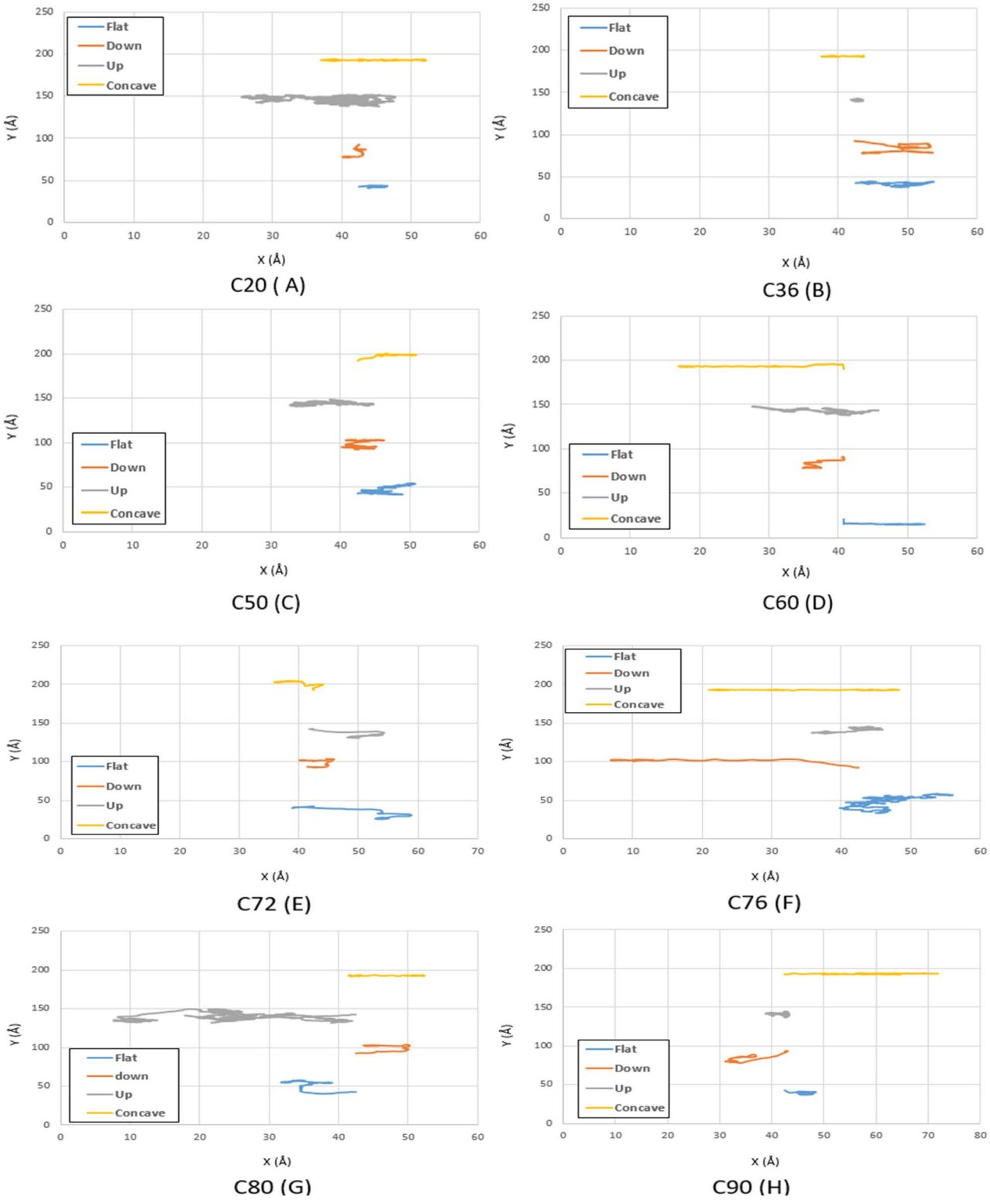

Figure 3. Trajectories of different fullerenes on a gold substrate at 75*K* for C_{20} (**A**), C_{36} (**B**), C_{50} (**C**), C_{60} (**D**), C_{72} (**E**), C_{76} (**F**), C_{80} (**G**), and C_{90} (**H** . The blue, red, black and yellow lines show the trajectories of the molecules on the flat, down side of the step, top side of the step, and concave substrates, respectively.

Contrary to the radius effects, increasing the temperature leads to a long-range movement for fullerenes due to increases in the internal energy of the molecules, which could overcome the non-bonded forces properly (Figs. 6, 7 and 8 blue and gray lines). Likewise, the downward step substrate has high-energy points, especially

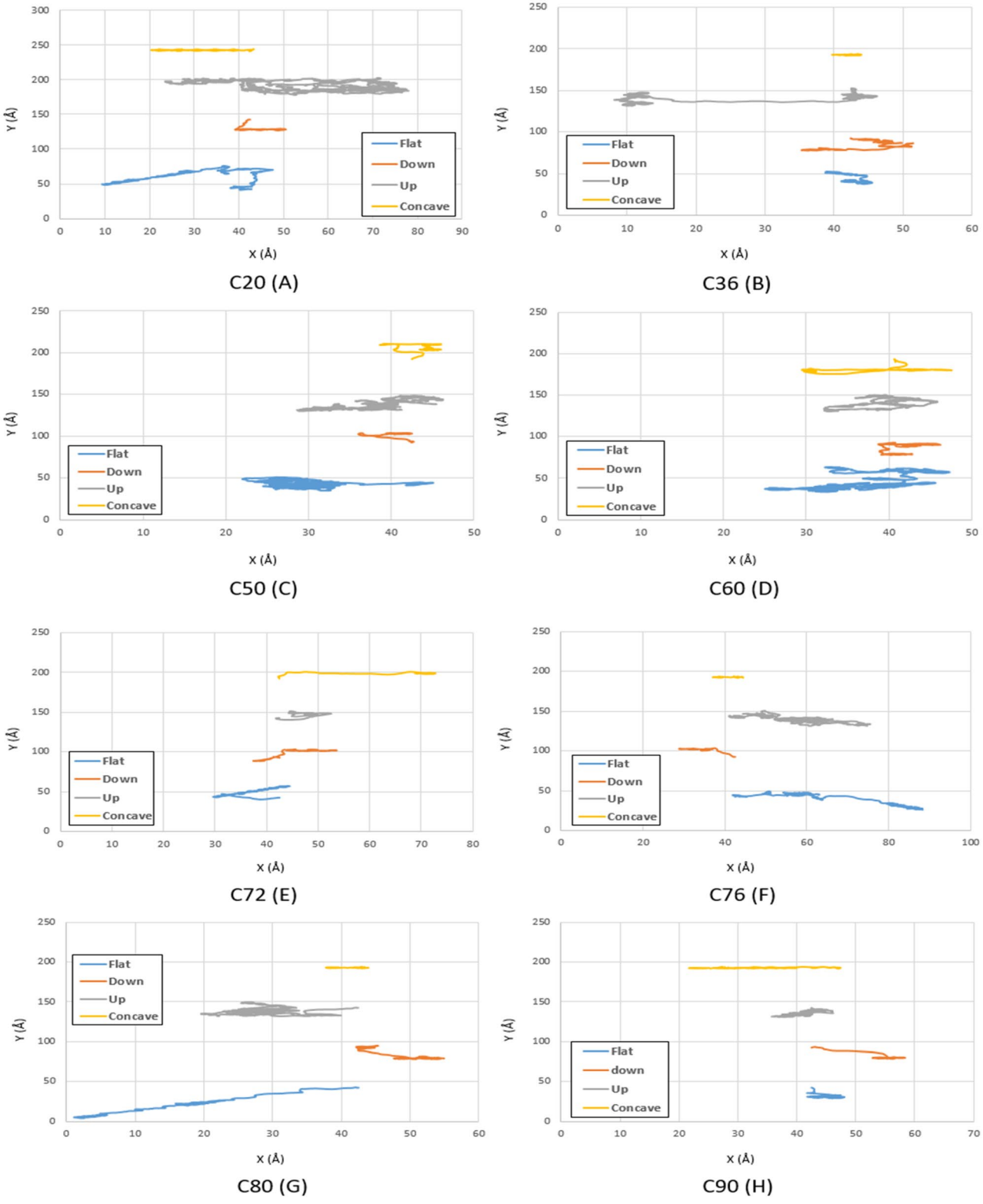

Figure 4. Trajectories of different fullerenes on a gold substrate at 150K for C_{20} (**A**), C_{36} (**B**), C_{50} (**C**), C_{60} (**D**), C_{72} (**E**), C_{76} (**F**), C_{80} (**G**), and C_{90} (**H**). The blue, red, black and yellow lines show the trajectories of the molecules on the flat, down side of the step, top side of the step, and concave substrates, respectively.

in the edges, which cause deviation of the molecules in this geometry. However, minimum energy is required for molecules to jump over the step; hence, fullerenes have shown less deviation on the downward step geometry

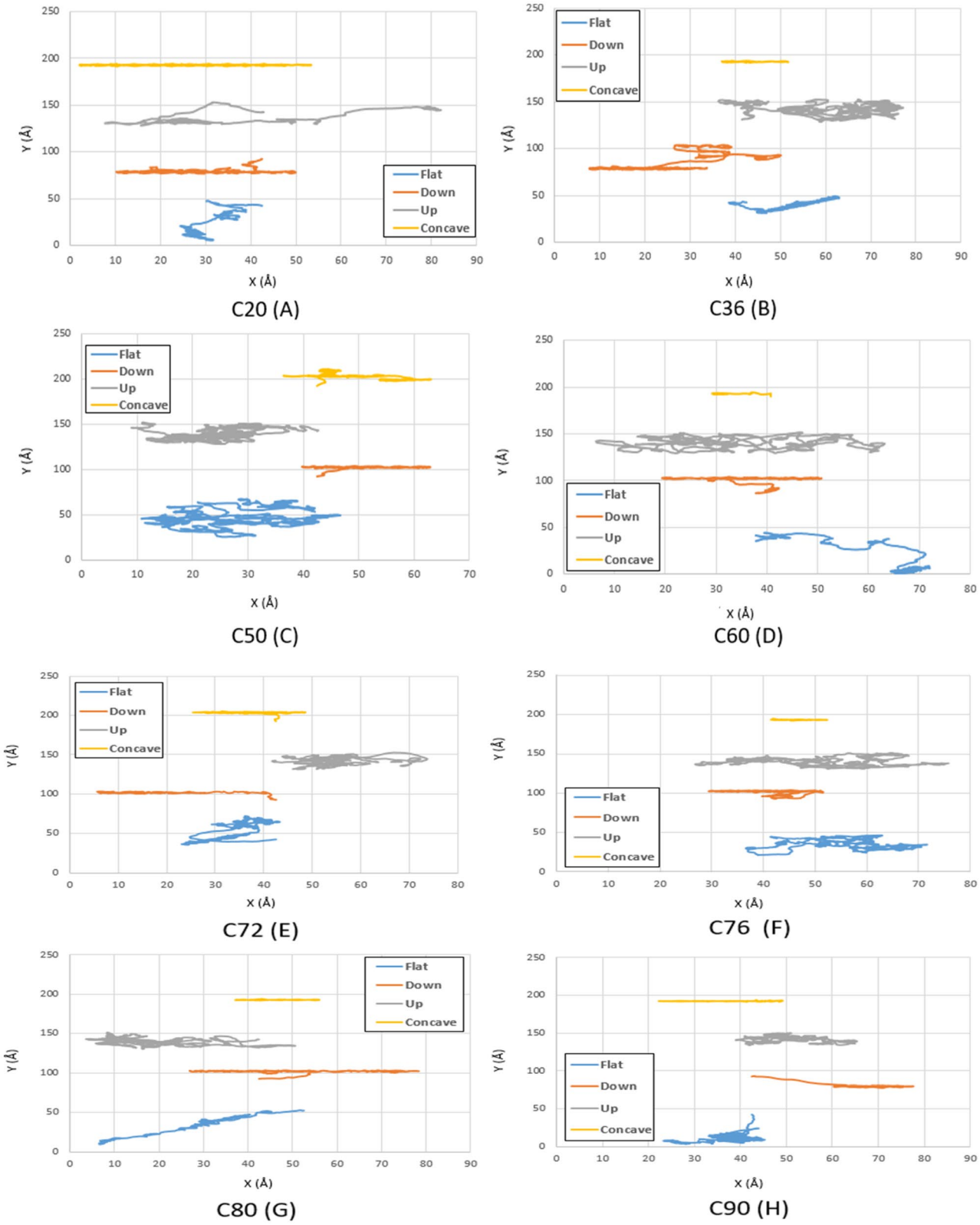

Figure 5. Trajectories of different fullerenes on a gold substrate at 300K for C_{20} (**A**), C_{36} (**B**), C_{50} (**C**), C_{60} (**D**), C_{72} (**E**), C_{76} (**F**), C_{80} (**G**), and C_{90} (**H**). The blue, red, black and yellow lines show the trajectories of the molecules on the flat, down side of the step, top side of the step, and concave substrates, respectively.

than the upward step geometry. At low temperatures, long-range movements were not observed so much so that all fullerenes were merely fluctuating (Figs. 3 and 4 red lines). As the fullerenes enlarge, the energy required to jump up the steps increases; thus, larger molecules could overcome the fluctuating motion and commence their motion at high temperatures with few deviations (Figs. 7 and 8 red lines). Besides, by increasing the radius of fullerene from C_{20} to C_{90}, the range of motion has increased on the downward step substrate. The same behavior has been repeated in the concave geometry. The higher the temperature, the greater range of fullerene motion was observed, especially when the radius and temperature increase simultaneously. It is worth mentioning that all fullerenes traveled a direct path at almost all temperatures due to several reasons. To begin with, the energy of fullerene molecules was devoted to climbing the gradual step form of the concave substrate. Second, due to the similar shape of the concave substrates and fullerenes, the movement of fullerenes is conducted in one direction. Third, Due to the fact that the concave substrate not only takes benefit of the long-range movement of fullerene on the flat substrate but also can successfully reduce the fullerene deviation because of the existence of a step-like surface on its both sides.

Moreover, a long-range movement has been observed for the concave substrate because of earlier mentioned reasons and the reciprocal effects of the temperature and radius on the motion of molecules, whose investigation is beyond the scope of this study (Figs. 3, 4, 5, and 6 yellow lines).

To investigate the behavior of fullerene molecules on different gold substrates, the energy of Lennard-Jones, the distance traveled, and the sliding velocity of each fullerene are presented in Figs. 9, 10, and 11, respectively. The sliding velocity has been considered since the main factor of fullerenes' movement is supplied by sliding motion rather than rolling motion.

The distance traveled by the molecules was increased as the temperature increased in all conditions (Fig. 9). In addition, a declining trend for the distance traveled by the molecules has been observed when the fullerenes' radius increased since as the fullerene enlarged, more carbon atoms interacted with the gold surface, slowing down the motion (Fig. 9). However, this decreasing trend for all temperatures has led to a constant value after C60 molecule. This stems from the fact that more carbon atoms were associated with the gold surface as the fullerene size increased, but their interactions will change slightly (Fig. 9).

As shown in Fig. 10, the higher the energy between the fullerenes and the gold surface, the less mobility was onbserved for fullerene molecules. Thus, the same Lennard-Jones potential energy for fullerenes on the flat, upward step, and downward step substrates has been observed. Concerning the concave substrate, less energy was observed due to the shape similarity of the gold surface and fullerenes (Fig. 10). However, C_{72} was the only exception, demonstrating the same potential energy on all the substrates due to its non-spherical shape.

The sliding velocity is one of the most important parameters for selecting fullerenes on different substrates, presented in Fig. 11 for all temperatures. As all the nanocars have been assembled with C_{60} wheels so far, only fullerenes indicated a better performance compared to C_{60} were investigated in the current study.

Given Fig. 3a, some of the fullerene molecules revealed more movements compared to C_{60} at $75K$, two of which are related to C_{76} on the downward step and concave substrates, and one of them is associated with C_{80} on the upward step substrate. Considering the aforementioned deviation results, The C_{76} molecule can be identified as the most desirable fullerene at $75K$.

At $150K$, despite the high mobility of C_{76} and C_{80} fullerenes on the flat substrate, they cannot be considered as alternative options due to the high amount of deviation on the flat substrate. Thus, C_{60} fullerene is considered as the best alternative for C_{60} at $150K$ due to its higher momentum compared to other fullerenes. However, for applications in which fullerenes move on concave-like geometries, C_{60} fullerene is still recommended (Fig. 11B).

Regarding Fig. 11C, C60 molecule did not perform properly at $300K$, and in accordance with the surface shape and mobility considerations, C_{76} molecule was introduced as the most suitable candidate at this temperature. It should be considered that the word "Candidate" was used for fullerenes that may have a better performance compared to C60 in different conditions.

At $400K$, C_{60} has shown insufficient performance on all the substrates except on the flat substrate in which considerable deviations limited all the applications. Hence, two of the fullerene molecules suggested, including C_{20} and C_{50}, revealed a good performance on the downward step and concave substrate, respectively. It should noted that C_{80} fullerene could also be considered a substitute for C_{50} molecule on concave geometry (Fig. 11D).

Although the performance of C_{60} molecule was unfavorable at $500K$, other molecules also have not offered a more satisfactory performance in all conditions. However, C_{20} and C_{60} molecules are recommended due to their better mobility to be utilized on the flat substrates despite the high deviations. In addition, C_{20} on the upward and downward step substrates, and C_{36} on the concave substrates are vigorously suggested, because of their stable motions with fewer deviations (Fig. 11E).

At 600K, C_{80} molecule indicated a proper performance on the upward step substrate and has been recognized as the leading candidate instead of C_{60}. After C_{80}, other fullerenes also showed an acceptable performance, including C_{20} on the flat and upward step substrates, C_{36} on the flat and downward step substrates, C_{50} on the flat and upward/downward step substrates, and C_{76} on the upward/downward step substrates (Fig. 11F).

As a result, Table 1 represents the most desirable fullerene on all substrates and at all temperatures. According to this, the required nano-machines can be designed appropriately to gain the best performance in different conditions. Moreover, C_{60} molecule, which was considered as a wheel in all nano-machines, could be a candidate among the fullerenes only in a few cases. Therefore, the presented study can be considered a compelling research in connection with introducing the most desirable fullerene molecules under different conditions.

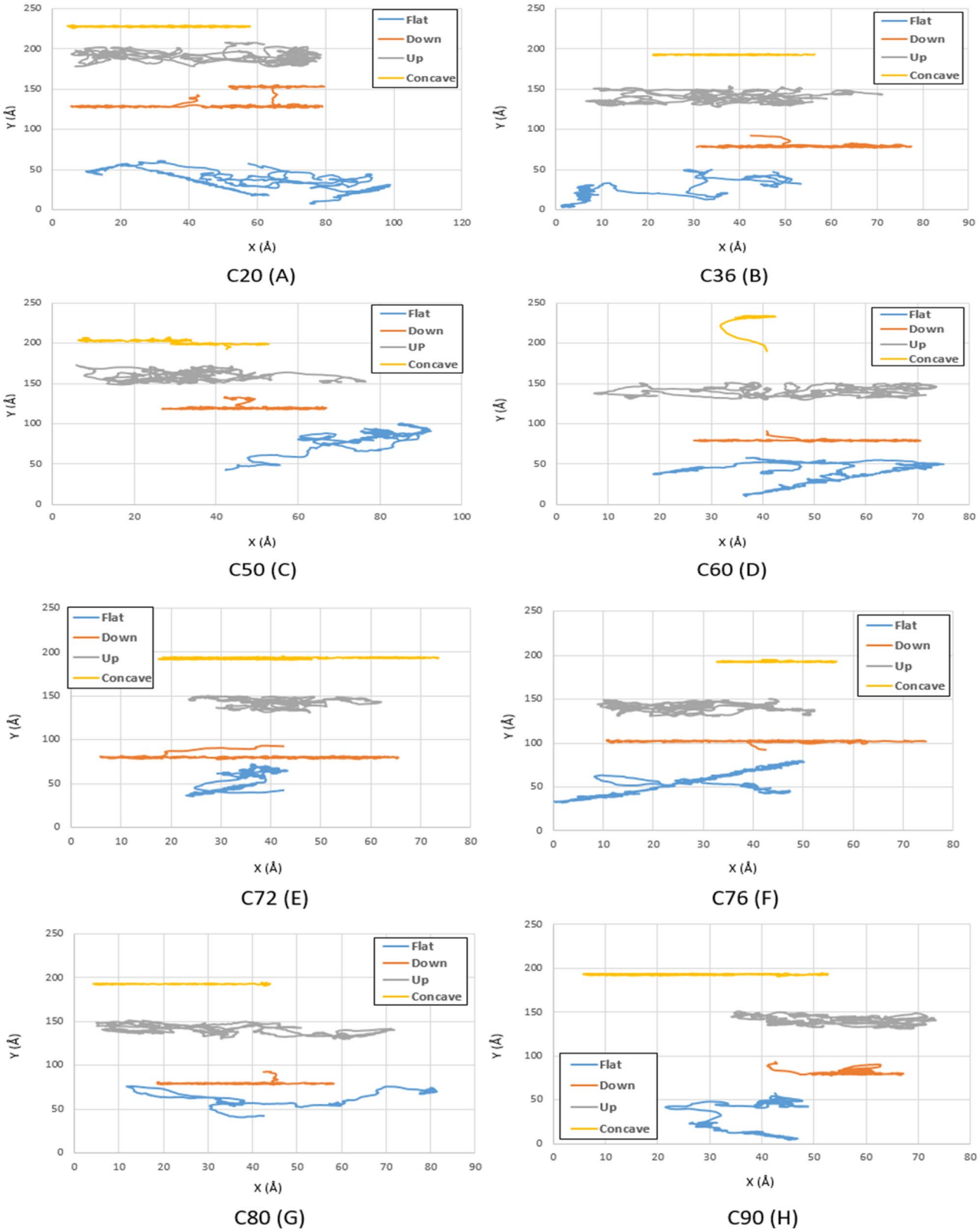

Figure 6. Trajectories of different fullerenes on a gold substrate at 400K for C_{20} (**A**), C_{36} (**B**), C_{50} (**C**), C_{60} (**D**), C_{72} (**E**), C_{76} (**F**), C_{80} (**G**), and C_{90} (**H**). The blue, red, black and yellow lines show the trajectories of the molecules on the flat, down side of the step, top side of the step, and concave substrates, respectively.

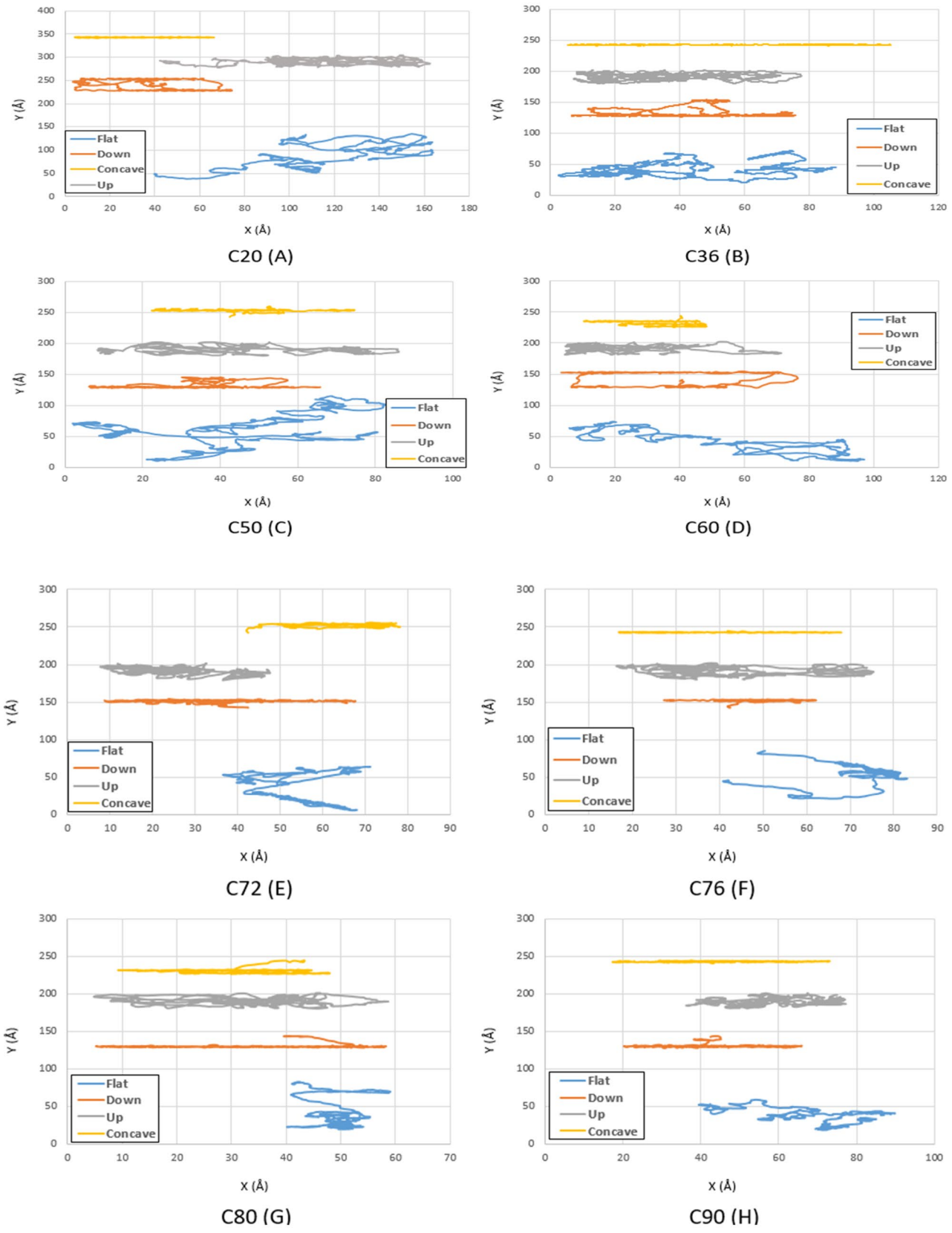

Figure 7. Trajectories of different fullerenes on a gold substrate at 500K for C_{20} (**A**), C_{36} (**B**), C_{50} (**C**), C_{60} (**D**), C_{72} (**E**), C_{76} (**F**), C_{80} (**G**), and C_{90} (**H**). The blue, red, black and yellow lines show the trajectories of the molecules on the flat, down side of the step, top side of the step, and concave substrates, respectively.

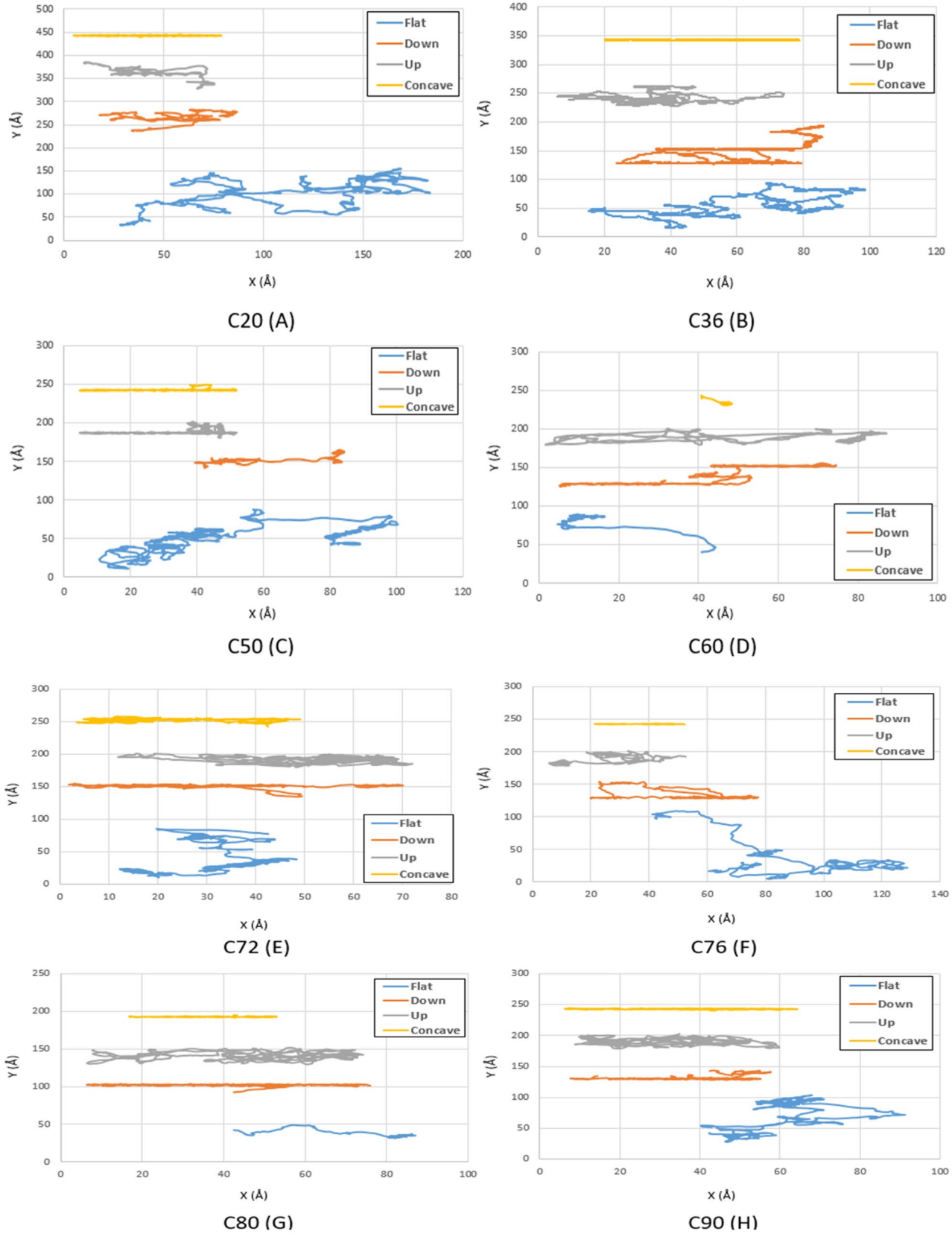

Figure 8. Trajectories of different fullerenes on a gold substrate at 600K for C_{20} (**A**), C_{36} (**B**), C_{50} (**C**), C_{60} (**D**), C_{72} (**E**), C_{76} (**F**), C_{80} (**G**), and C_{90} (**H**). The blue, red, black, and yellow lines show the trajectories of the molecules on the flat, down side of the step, top side of the step, and concave substrates, respectively.

Figure 9. Traveled distance by fullerenes on a gold substrate for 75K(**A**), 150K (**B**), 300K (**C**), 400K (**D**), 500K (**E**), and 600K (**F**). The blue, red, black and yellow bars show the traveled distant of the molecules on the flat, down side of the step, top side of the step, and concave substrates, respectively.

Conclusion

Simulation can be a valuable tool for investigating physical/chemical phenomena[37–42]. The current study investigates the different fullerenes' motion on a flat, upward step, downward step, and concave substrates at $75K$, $150K$, $300K$, $400K$, $500K$, and $600K$. For this aim, the C_{20}, C_{36}, C_{50}, C_{60}, C_{72}, C_{76}, C_{80}, and C_{90} fullerene molecules were chosen due to their shape and radius differences. Due to the fact that the nano-machine wheels play an important role in the nano-machine motion because they have the most interactions with the underneath substrate while they are connecting the nano-machine chassis. Hence, the current investigation can suggest optimal wheels for nano-machine movements and potentially improve the nano-machine performance for different applications.

As far as a straight-line movement is concerned, the fullerenes demonstrated the most deviation on the flat substrates compared to other substrates. At the same time, the concave, upward step, and downward step indicated fewer deviations due to their capability to restrict the unfavorable motions, respectively. Furthermore, as the temperature increased, the deviation of the fullerenes increased significantly except in the case of the concave substrate due to the restriction of fullerenes unlike the motion from both sides.

In the next stage, the effect of the radius on the fullerenes' motion was studied so that a long-range movement was observed for fullerenes on the concave substrate even at low temperatures ($75K$ and $150K$). However, the temperature has played a predominant role in the motion of the fullerene molecules on the flat, upward step, and downward step substrates.

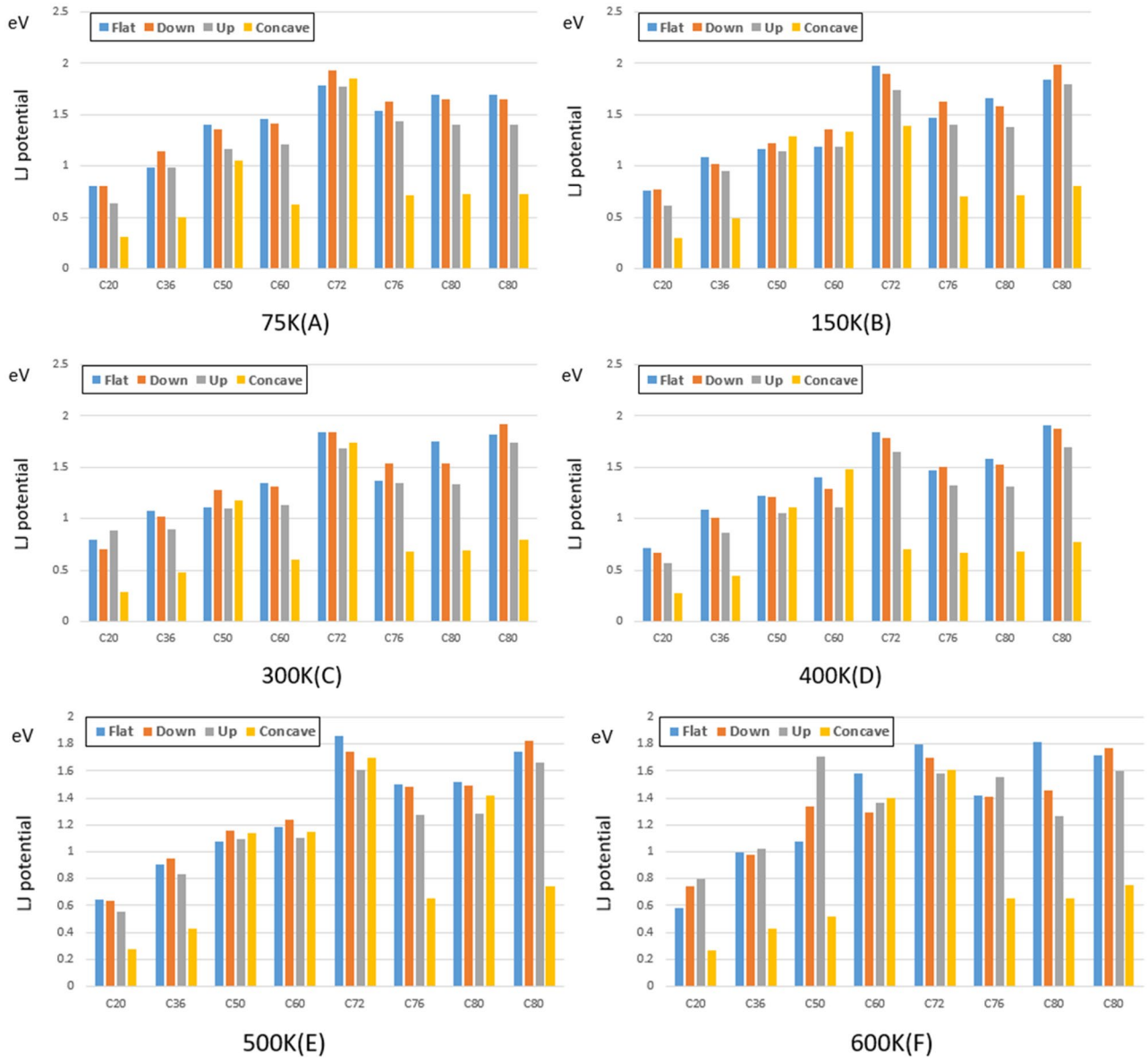

Figure 10. Lenard Jones potential energy for different fullerene molecules on a gold substrate for 75*K* (**A**), 150*K* (**B**), 300*K* (**C**), 400*K* (**D**), 500*K* (**E**), and 600*K* (**F**). The blue, red, black and yellow bars show Lenard Jones potential energy of the molecules on the flat, down side of the step, top side of the step, and concave substrates, respectively.

The Lennard-Jones potential has been employed to evaluate the Van Der Waals interaction forces between the fullerenes and the gold surfaces. The result indicates that fullerenes showed the same Lennard-Jones potential energy on the flat, upward step, and downward step substrates at a constant temperature since the gold surfaces interacting with the carbon atoms had an identical structure. Nonetheless, for the concave substrate, in the light of its shape resemblance with fullerenes, carbon atoms have more interactions with the gold surface, which leads to greater Lennard-Jones potential energy. Moreover, the Lennard-Jones potential differences between the concave geometry and the other substrates become more significant when the fullerenes radius increases (from C_{20} to C_{90}).

As previous studies stated, the temperature is the only effective characteristic of the distance traveled by the fullerenes, such that the surface changes did not influence the amount of the distance traveled. However, our findings revealed that as the radius increased, the distance traveled was decreased for the fullerenes at the same temperature. This stems from the fact that more carbon atoms were involved in the interaction with the gold surface, which slows the movement of fullerenes.

The sliding velocity parameter was also evaluated to determine the appropriate fullerenes according to probable nano-machines conditions (the dimension and temperature). To do so, more details are provided in Table 1, in which the candidate fullerenes are introduced considering the temperature and substrate changes. C_{60} molecule, which has been used as a wheel for nano-machines in almost all studies, was not recognized as a suitable candidate on the upward and downward step substrates at all temperatures. Besides, a better candidate was

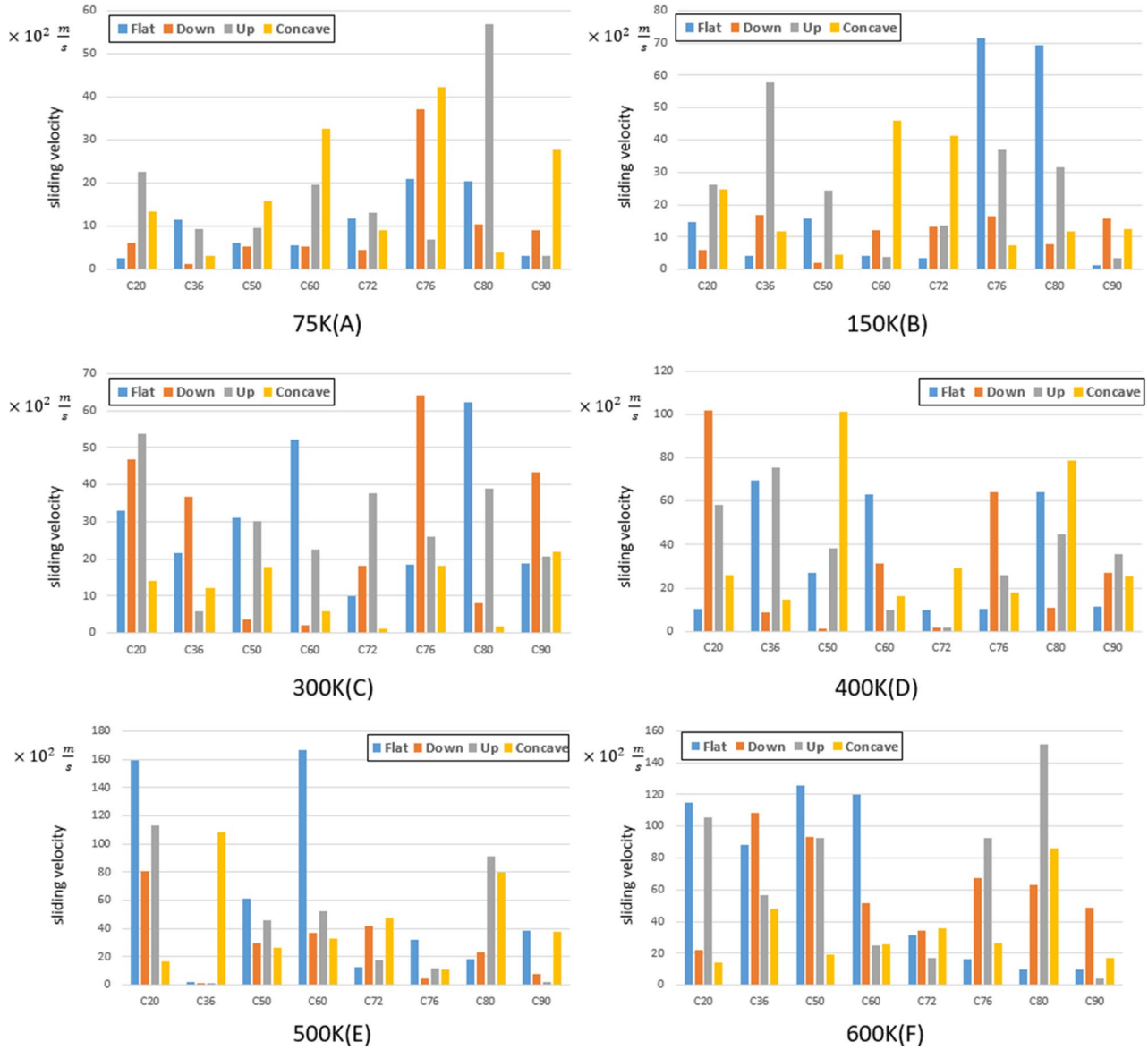

Figure 11. Sliding velocity for different fullerene molecules on a gold substrate for $75K$ (**A**), $150K$ (**B**), $300K$ (**C**), $400K$ (**D**), $500K$ (**E**) and $600K$ (**F**). The blue, red, black and yellow bars show sliding velocity of the molecules on the flat, down side of the step, top side of the step, and concave substrates, respectively.

	Flat	Up	Down	Concave
75 K	C76,C80	C80	C76	C76
150 K	C76,C80	C36	C36,C76,C90	C60
300 K	C60,C80	C20	C76	C50,C76,C90
400 K	C36,C60	C36	C20	C50
500 K	C20,C60	C20	C20	C36
600 K	C20,C50,C60	C80	C36,C50	C80

Table 1. Candidate fullerenes in different conditions.

introduced instead of C_{60} on the flat substrate at all temperatures. The concave substrate at $150K$ was the only case where no qualified candidate was discovered among our studied molecules. Our findings indicates that C_{60} is appropriate in less than 5% of fullerenes objectives. C_{20}, C_{76}, and C_{80} molecules have been candidates in most cases in different conditions, such that they were incompetent only in seven situations, which is mentioned in the result section. In addition, the C_{72} molecule was the only fullerene that was not introduced as a candidate due to

its cylindrical structure, which caused the molecule to fall on its more extensive cross-section after a period. All in all, our investigation helps to understand the optimal performance of different fullerene molecules on gold substrates in order to find their probable application, especially in nano-machines objectives.

Data availability

The data of this study is available upon reasonable request from the corresponding author.

Received: 19 March 2022; Accepted: 18 August 2022
Published online: 24 August 2022

References

1. Samorì, P. Scanning probe microscopies beyond imaging. *J. Mater. Chem.* **14**(9), 1353–1366. https://doi.org/10.1039/B314626J (2004).
2. Vives, G. & Tour, J. M. Synthesis of single-molecule nanocars. *Acc. Chem. Res.* **42**(3), 473–487. https://doi.org/10.1021/ar8002317 (2009).
3. Alberts, B. The cell as a collection of protein machines: Preparing the next generation of molecular biologists. *Cell* **92**(3), 291–294. https://doi.org/10.1016/S0092-8674(00)80922-8 (1998).
4. Kinbara, K. & Aida, T. Toward intelligent molecular machines: directed motions of biological and artificial molecules and assemblies. *Chem. Rev.* **105**(4), 1377–1400. https://doi.org/10.1021/cr030071r (2005).
5. Shirai, Y. *et al.* Surface-rolling molecules. *J. Am. Chem. Soc.* **128**(14), 4854–4864. https://doi.org/10.1021/ja058514r (2006).
6. Chu, P.-L.E. *et al.* Synthesis and single-molecule imaging of highly mobile adamantane-wheeled nanocars. *ACS Nano* **7**(1), 35–41. https://doi.org/10.1021/nn304584a (2013).
7. Sasaki, T., Osgood, A. J., Alemany, L. B., Kelly, K. F. & Tour, J. M. Synthesis of a Nanocar with an angled chassis. Toward circling movement. *Org. Lett.* **10**(2), 229–232. https://doi.org/10.1021/ol702642r (2008).
8. Sasaki, T. & Tour, J. M. Synthesis of a dipolar nanocar. *Tetrahedron Lett.* **48**(33), 5821–5824. https://doi.org/10.1016/j.tetlet.2007.06.080 (2007).
9. Shirai, Y., Osgood, A. J., Zhao, Y., Kelly, K. F. & Tour, J. M. Directional control in thermally driven single-molecule nanocars. *Nano Lett.* **5**(11), 2330–2334. https://doi.org/10.1021/nl051915k (2005).
10. Sasaki, T., Morin, J.-F., Lu, M. & Tour, J. M. Synthesis of a single-molecule nanotruck. *Tetrahedron Lett.* **48**(33), 5817–5820. https://doi.org/10.1016/j.tetlet.2007.06.081 (2007).
11. Morin, J.-F., Sasaki, T., Shirai, Y., Guerrero, J. M. & Tour, J. M. Synthetic routes toward carborane-wheeled nanocars. *J. Org. Chem.* **72**(25), 9481–9490. https://doi.org/10.1021/jo701400t (2007).
12. Lohrasebi, A., Neek-Amal, M. & Ejtehadi, M. R. Directed motion of C60 on a graphene sheet subjected to a temperature gradient. *Phys. Rev. E* **83**(4), 042601. https://doi.org/10.1103/PhysRevE.83.042601 (2011).
13. Cuberes, M. T., Schlittler, R. R. & Gimzewski, J. K. Room-temperature repositioning of individual C 60 molecules at Cu steps: Operation of a molecular counting device. *Appl. Phys. Lett.* **69**(20), 3016–3018. https://doi.org/10.1063/1.116824 (1996).
14. Neek-Amal, M., Abedpour, N., Rasuli, S. N., Naji, A. & Ejtehadi, M. R. Diffusive motion of on a graphene sheet. *Phys. Rev. E* **82**(5), 051605. https://doi.org/10.1103/PhysRevE.82.051605 (2010).
15. Martsinovich, N. & Kantorovich, L. Modelling the manipulation of C 60 on the Si(001) surface performed with NC-AFM. *Nanotechnology* **20**(13), 135706. https://doi.org/10.1088/0957-4484/20/13/135706 (2009).
16. Ozmaian, M., Fathizadeh, A., Jalalvand, M., Ejtehadi, M. R. & Allaei, S. M. V. Diffusion and self-assembly of C60 molecules on monolayer graphyne sheets. *Sci. Rep.* **6**(1), 21910. https://doi.org/10.1038/srep21910 (2016).
17. Ahangari, M. G., Ganji, M. D. & Jalali, A. Interaction between fullerene-wheeled nanocar and gold substrate: A DFT study. *Phys. E Low-dimens. Syst. Nanostruct.* **83**, 174–179. https://doi.org/10.1016/j.physe.2016.05.029 (2016).
18. Vaezi, M., Nejat Pishkenari, H. & Nemati, A. Mechanism of C 60 rotation and translation on hexagonal boron-nitride monolayer. *J. Chem. Phys.* **153**(23), 234702. https://doi.org/10.1063/5.0029490 (2020).
19. Wang, L. & Xu, Z. A graphene-based nanoparticle motion converter. *Int. Core J. Eng.* **5**(1), 114–118 (2019).
20. Zhang, J. *et al.* Investigating the motion of molecular machines on surfaces by STM: The nanocar and beyond. In *2007 7th IEEE Conference on Nanotechnology (IEEE NANO)*, 243–246 (2007). Doi: https://doi.org/10.1109/NANO.2007.4601180.
21. Kelly, K. Probing molecular machines on surfaces: The nanocar and beyond. *Microsc. Microanal.* **14**(S2), 956–957. https://doi.org/10.1017/S1431927608085176 (2008).
22. Grill, L. ChemInform abstract: Functionalized molecules studied by STM: Motion, switching and reactivity. *ChemInform* https://doi.org/10.1002/chin.200823260 (2008).
23. Shamloo, A. *et al.* Modeling of an ultrasound system in targeted drug delivery to abdominal aortic aneurysm: A patient-specific in silico study based on ligand-receptor binding. *IEEE Trans. Ultrason. Ferroelectr. Freq. Control* **69**(3), 967–974. https://doi.org/10.1109/TUFFC.2021.3138868 (2022).
24. Forouzandehmehr, M., Ghoytasi, I., Shamloo, A. & Ghosi, S. Particles in coronary circulation: A review on modelling for drug carrier design. *Mater. Des.* **216**, 110511. https://doi.org/10.1016/j.matdes.2022.110511 (2022).
25. Ebrahimi, S., Vatani, P., Amani, A. & Shamloo, A. Drug delivery performance of nanocarriers based on adhesion and interaction for abdominal aortic aneurysm treatment. *Int. J. Pharm.* **594**, 120153. https://doi.org/10.1016/j.ijpharm.2020.120153 (2021).
26. Shamloo, A., Nejad, M. A. & Saeedi, M. Fluid–structure interaction simulation of a cerebral aneurysm: Effects of endovascular coiling treatment and aneurysm wall thickening. *J. Mech. Behav. Biomed. Mater.* **74**, 72–83. https://doi.org/10.1016/j.jmbbm.2017.05.020 (2017).
27. Shamloo, A., Manuchehrfar, F. & Rafii-Tabar, H. A viscoelastic model for axonal microtubule rupture. *J. Biomech.* **48**(7), 1241–1247. https://doi.org/10.1016/j.jbiomech.2015.03.007 (2015).
28. Akimov, A. V., Nemukhin, A. V., Moskovsky, A. A., Kolomeisky, A. B. & Tour, J. M. Molecular dynamics of surface-moving thermally driven nanocars. *J. Chem. Theory Comput.* **4**(4), 652–656. https://doi.org/10.1021/ct7002594 (2008).
29. Konyukhov, S. S. *et al.* Rigid-body molecular dynamics of fullerene-based nanocars on metallic surfaces. *J. Chem. Theory Comput.* **6**(9), 2581–2590. https://doi.org/10.1021/ct100101y (2010).
30. Konyukhov, S. S. *et al.* Diffusion of fullerene-based nanocars on the surface of a gold crystal. *Moscow Univ. Chem. Bull.* **65**(4), 219–220. https://doi.org/10.3103/S0027131410040012 (2010).
31. Asadollahi, D. & Shariati, M. Investigation of shear forces in twisted carbon nanotube bundles using a structural mechanics approach. *Acta Mech.* **232**(6), 2425–2441. https://doi.org/10.1007/s00707-021-02949-y (2021).
32. Nejat Pishkenari, H., Nemati, A., Meghdari, A. & Sohrabpour, S. A close look at the motion of C60 on gold. *Curr. Appl. Phys.* **15**(11), 1402–1411. https://doi.org/10.1016/j.cap.2015.08.003 (2015).
33. Foiles, S. M., Baskes, M. I. & Daw, M. S. Embedded-atom-method functions for the fcc metals Cu, Ag, Au, Ni, Pd, Pt, and their alloys. *Phys. Rev. B* **33**(12), 7983–7991. https://doi.org/10.1103/PhysRevB.33.7983 (1986).

34. Plimpton, S. Fast parallel algorithms for short-range molecular dynamics. *J. Comput. Phys.* **117**(1), 1–19. https://doi.org/10.1006/jcph.1995.1039 (1995).
35. Humphrey, W., Dalke, A. & Schulten, K. VMD: Visual molecular dynamics. *J. Mol. Graph.* **14**(1), 33–38. https://doi.org/10.1016/0263-7855(96)00018-5 (1996).
36. Yu, T.-Q., Alejandre, J., López-Rendón, R., Martyna, G. J. & Tuckerman, M. E. Measure-preserving integrators for molecular dynamics in the isothermal–isobaric ensemble derived from the Liouville operator. *Chem. Phys.* **370**(1–3), 294–305. https://doi.org/10.1016/j.chemphys.2010.02.014 (2010).
37. Ebrahimi, S. & Fallah, F. Investigation of coronary artery tortuosity with atherosclerosis: A study on predicting plaque rupture and progression. *Int. J. Mech. Sci.* **223**, 107295. https://doi.org/10.1016/j.ijmecsci.2022.107295 (2022).
38. Alishiri, M., Ebrahimi, S., Shamloo, A., Boroumand, A. & Mofrad, M. R. K. Drug delivery and adhesion of magnetic nanoparticles coated nanoliposomes and microbubbles to atherosclerotic plaques under magnetic and ultrasound fields. *Eng. Appl. Comput. Fluid Mech.* **15**(1), 1703–1725. https://doi.org/10.1080/19942060.2021.1989042 (2021).
39. Manzoori, A., Fallah, F., Sharzehee, M. & Ebrahimi, S. Computational investigation of the stability of stenotic carotid artery under pulsatile blood flow using a fluid-structure interaction approach. *Int. J. Appl. Mech.* **12**(10), 2050110. https://doi.org/10.1142/S1758825120501100 (2020).
40. Shamloo, A. & Sarmadi, M. Investigation of the adhesive characteristics of polymer–protein systems through molecular dynamics simulation and their relation to cell adhesion and proliferation. *Integr. Biol.* **8**(12), 1276–1295. https://doi.org/10.1039/c6ib00159a (2016).
41. Shamloo, A., Mohammadaliha, N. & Mohseni, M. Integrative utilization of microenvironments, biomaterials and computational techniques for advanced tissue engineering. *J. Biotechnol.* **212**, 71–89. https://doi.org/10.1016/j.jbiotec.2015.08.005 (2015).
42. Shamloo, A., Pedram, M. Z., Heidari, H. & Alasty, A. Computing the blood brain barrier (BBB) diffusion coefficient: A molecular dynamics approach. *J. Magn. Magn. Mater.* **410**, 187–197. https://doi.org/10.1016/j.jmmm.2016.03.030 (2016).

Acknowledgements

This research did not receive any specific grant from funding agencies in the public, commercial, or not-for-profit sectors.

Author contributions

A.S. Designed the simulations, analyzed the data, supervised the project and wrote the paper. M.A.B. Designed and performed the simulations, analyzed the data, and wrote the paper. M.T. Designed and performed the simulations, analyzed the data, and wrote the paper. S.S. Designed and performed the simulations, analyzed the data, and wrote the paper.

Competing interests

The authors declare no competing interests.

Additional information

Correspondence and requests for materials should be addressed to A.S.

Reprints and permissions information is available at www.nature.com/reprints.

Publisher's note Springer Nature remains neutral with regard to jurisdictional claims in published maps and institutional affiliations.